

Tunable fluid-filled phononic metastrip

Ting-Ting Wang, Yan-Feng Wang, Yue-Sheng Wang, and Vincent Laude

Citation: *Appl. Phys. Lett.* **111**, 041906 (2017); doi: 10.1063/1.4985167

View online: <http://dx.doi.org/10.1063/1.4985167>

View Table of Contents: <http://aip.scitation.org/toc/apl/111/4>

Published by the [American Institute of Physics](#)



CiSE magazine is
an innovative blend.

Tunable fluid-filled phononic metastrip

Ting-Ting Wang,¹ Yan-Feng Wang,^{1,a)} Yue-Sheng Wang,¹ and Vincent Laude^{2,b)}

¹*Institute of Engineering Mechanics, Beijing Jiaotong University, 100044 Beijing, China*

²*Institut FEMTO-ST, Université Bourgogne Franche-Comté, CNRS, 25030 Besançon, France*

(Received 26 May 2017; accepted 18 July 2017; published online 28 July 2017)

We study the propagation of Lamb waves in a one-dimensional tunable phononic metastrip composed of a periodic sequence of hollow pillars that can be selectively filled with water. Band structures and transmission properties are computed numerically for metastrips with different fluid fillings by using the finite element method. Good agreement is observed with experimental results obtained with an aluminum metastrip. In particular, it is found that the frequency range of bandgaps and passbands can be controlled through fluid filling. Our results imply that Lamb waves in the solid metastrip can be harnessed through changing the properties of the pillars via fluid-solid interaction. The work in this paper is relevant to practical design of tunable acoustic devices. *Published by AIP Publishing.* [<http://dx.doi.org/10.1063/1.4985167>]

Phononic crystals (PCs) are a kind of functional composite possessing some form of spatial periodicity.^{1,2} It may generate bandgaps, within which the propagation of acoustic/elastic waves is completely forbidden. During the last decade, a great deal of effort has been made to control the propagation of elastic waves in PCs.³ PCs are found to have a variety of potential applications,⁴ such as filters,⁵ sensors,^{6,7} waveguides,⁸ or high frequency resonators.^{9,10}

In recent years, there has been growing interest in one-dimensional (1D) phononic strips possessing a wide bandgap at low frequencies.¹¹ Wave propagation in a 1D strip is indeed different from that in a 2D PC thin plate, due to the fact that there are additional free boundaries along the strip.¹² Actually, these structures present a potential for use as anchor loss reduction in resonators,¹³ vibration isolation,¹⁴ or multi-frequency Lamb wave filters.¹⁵ Hsu *et al.*¹⁶ investigated the effects of different ways of cutting the strip on the band structures and transmission properties. Pennec *et al.*¹⁷ investigated strips sustaining dual phononic and phononic bandgaps; Hatanaka *et al.*¹⁸ demonstrated the ability to switch the mechanical vibration from the strip to a cavity; Coffy *et al.*¹⁹ showed evidence of a broad bandgap at low frequencies originating from the vibration of pillars connected to the strip via a soft layer. Although these works provide a promising approach to control the propagation of elastic waves, the resulting structures and material parameters can hardly be changed.^{20,21} In other words, a solid phononic strip is hardly tunable or reconfigurable. In the field of PCs, numerous works have been devoted to the design and development of tunable PCs, for example, by using material, geometric nonlinearity,²² or external field control,²³ though such approaches require components with active properties and power consumption. Tunability, in contrast, is more easily realized by using solid/fluid PCs or sonic crystals.²⁴ The propagation of acoustic waves in a fluid medium has for instance been controlled through changing the properties of the solid inclusions.²⁵ Conversely, elastic waves in a solid-

matrix system can be manipulated through changing the properties of fluid fillings.^{26,27} However, almost all investigations in this direction have been limited to numerical demonstrations.

In the present work, we fabricate a phononic metastrip consisting of a periodic sequence of hollow pillars grafted onto a strip perforated with periodic rectangular holes. Tunability is realized by filling the hollow pillars selectively with a fluid. First, we investigate the dispersion relations and the transmission properties of metastrips whose pillars are either empty or fully filled. We show that transmission in certain frequency ranges can be switched on and off by fluid filling, i.e., the position of passbands and stopbands can be adjusted. Next, we focus on the point-defect fluid-filled cavity. It is found that the resonating cavity can quench energy transmission through the strip. Finally, we examine the modification of spectral transmission as the number of fluid-filled cavities is increased.

The manufactured sample is shown in Fig. 1(a). The chosen solid and fluid materials are isotropic aluminum 6061 (mass density $\rho_s = 2700 \text{ kg/m}^3$, Poisson's ratio $\nu = 0.33$, and Young's modulus $E = 68.9 \text{ GPa}$) and water (mass density $\rho_f = 1000 \text{ kg/m}^3$ and sound velocity $c = 1490 \text{ m/s}$), respectively. The unit cell is composed of one pillar grafted onto a perforated plate forming a strip, as depicted in Fig. 1(b). This phononic strip generates complete bandgaps in the relatively low frequency range.²⁸ Measurements are conducted by using a Polytec-PSV-500 scanning vibrometer, as illustrated by Fig. 1(c). A periodic chirp is chosen as the source waveform. It is amplified by the power amplifier before it is applied to the sample. The amplified signal is transformed to a displacement vibration signal via a piezoelectric patch bonded on one side of the sample. The transmitted vertical displacement signal is recorded by the vibrometer at the other side of the sample.

To evaluate numerically the transmission properties, we built a 3D finite element model. Acoustic-structure boundary conditions are applied at the interface between fluid and solid, and a sound-soft boundary condition is applied on the top surface of the liquid column when fluid is filled. Dispersion curves are then calculated by using Bloch-Floquet

^{a)}Electronic mail: wangyanfeng@bjtu.edu.cn

^{b)}Electronic mail: vincent.laude@femto-st.fr

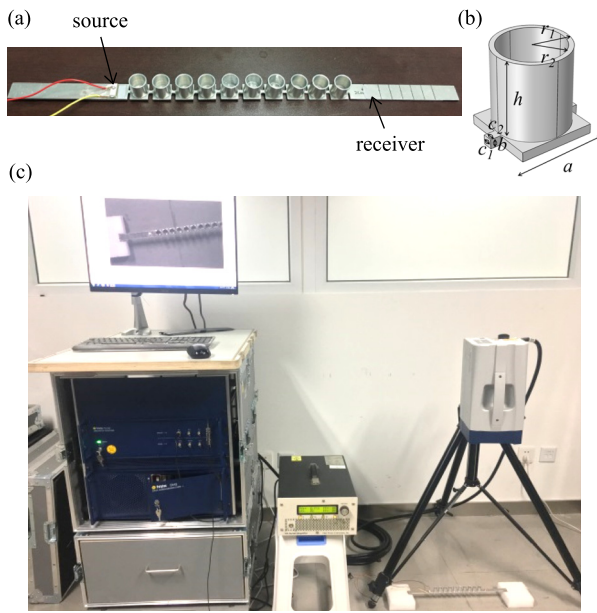


FIG. 1. (a) A finite 1D phononic metastrip aluminum sample consisting of ten hollow pillars bonded on a strip. (b) Schematic of the PC unit cell. Geometrical parameters used in this paper are $a = 2\text{ cm}$, $h = 0.8a$, $b = c_1 = 0.1a$, $r_1 = 0.38a$, $r_2 = 0.33a$, and $c_2 = 0.11a$. (c) Photograph of the experimental setup.

periodic boundary conditions. Numerical transmission is further calculated by considering a finite metastrip with ten unit cells, sandwiched between an ingoing and an outgoing homogeneous medium. Perfectly matched layers (PMLs) are added to both ends of the metastrip to avoid reflections. A wave source of z -polarization with displacement amplitude U_{z0} is applied on the left homogeneous part of the metastrip. The transmitted displacements are recorded on the right homogeneous part. We then evaluate the transmission by considering the ratio of the z -component of the displacements integrated over the two homogeneous parts.

Numerical and experimental results for the hollow pillars either all empty or all filled with water are shown in Fig. 2. The figure presents the band structures for the infinite and periodic strip, the transmissions computed for a 10-pillar long strip, and the transmissions measured with the sample of Fig. 1. Color information was added to the band structures to represent the polarization amount of the z -component of the displacement.²⁹ Particular frequency ranges where transmission can be switched on and off by fluid filling are highlighted in grey. In order to allow for a fair comparison between numerical and experimental transmission, a “noise floor” was added to the numerical results in order to limit the minimum of transmission to -86 dB .

Lamb waves in the phononic strip are confined in the supporting plate, are periodically loaded with the fluid, and hybridize with internal resonances of the unit-cell. Consequently, band structures are composed of both dispersive bands and nearly flat bands. It should be noted that resonances can be concentrated either on the pillar or on the four corners of the supporting plate, as shown in Fig. 2(c₁). Numerical results indicate that flat bands can cause sharp transmission peaks, but these are only faintly present in the experiment. This discrepancy may be caused by the absence of loss in the finite element model, which may lead to damped resonances. Furthermore, the numerical model does not take account of the exact properties of the actual sample. For example, the support of the metastrip during experiments and the inhomogeneity of the excitation source are not considered. The passbands and bandgaps defined by dispersive bands are in contrast clearly observed in the experimental transmissions. They are globally consistent with the numerical transmissions, except for a slight frequency shift that can be attributed a slightly inaccurate modelling of the sample geometry and material properties. In addition, nearly no qualitative change appears in the transmission if a symmetric excitation is applied, as we checked experimentally. As a

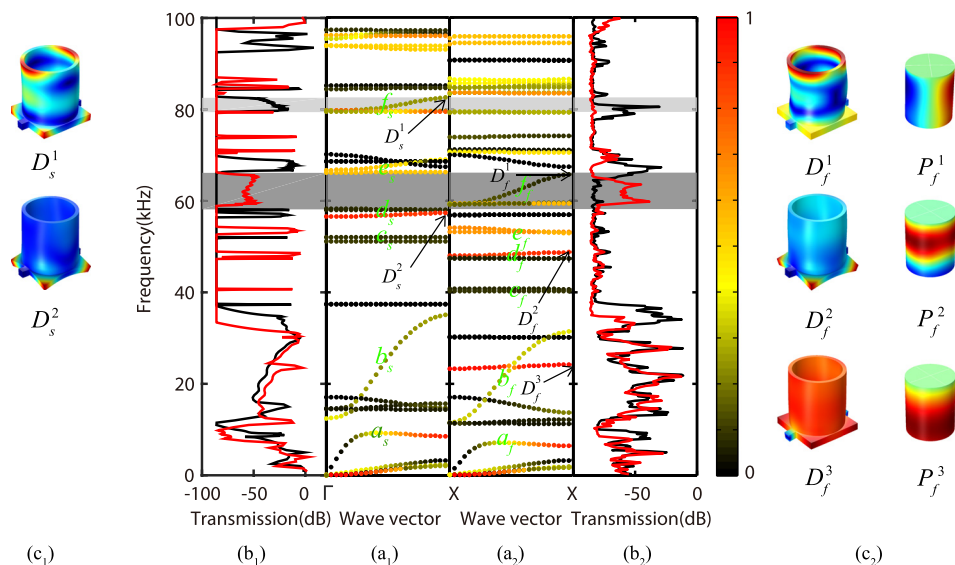


FIG. 2. Phononic band structure of a metastrip (a₁) without and (a₂) with water filling the hollow pillars. (b₁) Numerical and (b₂) experimental transmission spectra for a finite metastrip with 10 pillars without (black line) or with (red line) water. The gray and light gray frequency ranges highlight particular bandgaps and passbands discussed in the text. The color scale is for the polarization amount of the z -component of displacement. Eigenmodes at selected points are shown (c₁) without and (c₂) with water filling. The total displacement is shown in both cases and pressure is added in the case of water filling. Blue (red) corresponds to zero (maximum) amplitude for the displacement field but to negative (positive) amplitude for the case of pressure.

note, since the structure is not symmetrical with respect to a horizontal plane, bending and torsional modes are always coupled.

The dispersion of passing bands is strongly affected by the presence or absence of water inside the pillars. In general, it is observed that the band structure is compressed, i.e., all bands shift down to lower frequencies. In order to understand this phenomenon, we consider specifically the in-plane bands a , b , c , d , e , and f in Fig. 2. By in-plane bands, we mean that the displacements for the corresponding Bloch waves are mostly in the plane of the supporting strip. The modifications introduced by the addition of water can be tracked by observing modal shapes. Indeed, considering vibration modes at points D_s^2 and D_f^2 of band e , for example, it can be observed that the displacement distributions in the solid part are almost the same, while elasto-acoustic coupling with the second resonance of the water column brings the frequency down. As a consequence of the frequency downshift, bandgaps become narrower and their central frequencies decrease. Remarkably, the introduction of water enhances the propagation of Lamb waves in the frequency range from 58.5 kHz to 66 kHz where a bandgap was initially present. Concurrently, a bandgap appears in the frequency range from 79.4 kHz to 82.5 kHz where transmission was previously permitted by the presence of the dispersive band labelled f . Observing the modal shapes, it can be concluded that the downshift of band f in the presence of water is indeed the cause of the interchange of bandgaps and passbands. This effect suggests potential applications to the tuning of Lamb wave bandgaps.

Moreover, it can be observed that additional modes are created when water is added. An example is the band supporting the Bloch wave labelled D_f^2 . The pressure distribution for this Bloch wave shown in Fig. 2(c₂) reveals that water undergoes vertical vibrations that are similar to that of the first resonance of an isolated water cylinder. This example also implies that different fluid resonances have different coupling strengths with Lamb waves in the solid matrix.

We checked that the frequency shift of passbands that we observe cannot be simply attributed to a local-resonance mechanism. Hybridization of a local resonance with a propagating band generally leads to the formation of avoided crossings around the local resonance frequency but not to a shift of the dispersion of the propagating band. In order to verify this point, we replaced the fluid by an additional solid mass distributed either only in the base of the pillar or in the base of the pillar as well as in the pillar wall. The corresponding dispersion curves are shown in Fig. 3. In the first case, only avoided crossings appear; in the second case, band shifts are produced as well, similarly to the case of fluid filling. The two situations, distributed solid mass and distributed fluid load, are however not equivalent: even though the added masses are the same, acoustoelastic coupling brings in specific features, as we noted above. An important practical difference, furthermore, is that continuously tuning the volume of a fluid is arguably easier than continuously tuning a solid mass.

We explain the downshift of the propagating bands as follows. Thanks to the fluid-solid boundary condition inside the cup, Lamb waves in the solid strip are partly

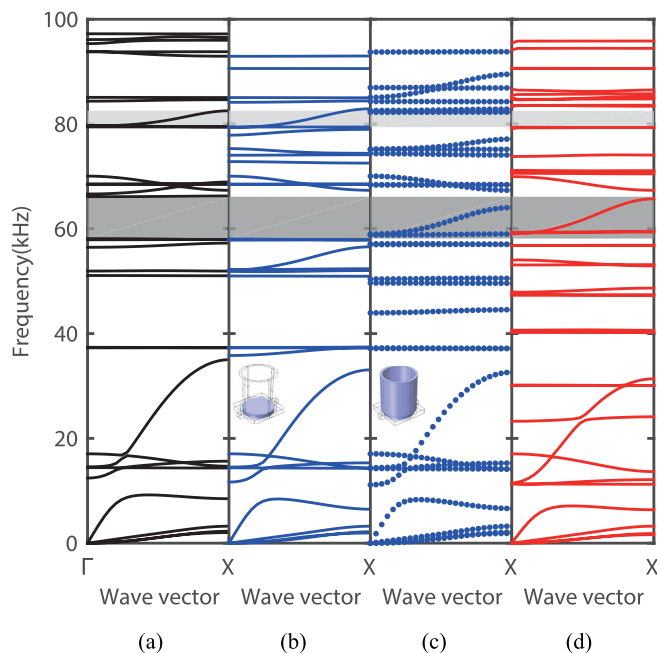


FIG. 3. Modification of the phononic band structure of the metastrip under different ways of adding the same amount of mass to the pillars. The band structure is shown (a) without added mass, (b) for solid mass distributed in the base of pillar, (c) for solid mass distributed in the base of the pillar as well as in the pillar wall, and (d) for water filling the pillar. The insets in (b) and (c) show the regions where mass is added.

converted to pressure waves in water. The pressure waves in water decompose on the modes available at the particular frequency of excitation, as the volume of water is finite and closed by definite boundary conditions. For most frequencies, however, the conversion is not resonant. Back-conversion to Lamb waves in the solid occurs with a certain delay, causing an apparent slowing down of the propagation of Lamb waves along the strip. As the phase velocity is reduced, the dispersion of propagating bands is effectively shifted downward in frequency for a given wavenumber.

Next, we focus on wave propagation in the metastraps with a defect. A point-defect cavity is created by filling the fifth pillar only with water. Figure 4 shows the modification of the band structure and of the transmission when water is added. It can be clearly observed that additional bands, corresponding to defect modes, appear inside the complete bandgaps of the perfect system. Although there is apparently only a slight change in the spectral transmission upon introducing one defect, transmission properties are quantitatively affected. For example, the transmission at frequency 81 kHz, labelled P in Fig. 4(a₁), decreases by almost 20 dB when the defect cavity is introduced. This transmission decrease stands for nearly one order of magnitude decrease of the displacement amplitude at the end of the metastrip. Displacement fields in the perfect and defect metastraps are displayed in Figs. 4(b) and 4(c), respectively. We observe that all hollow pillars vibrate along the perfect metastrip, as expected for a passing band in the dispersion curve. In contrast, wave propagation is quenched by the cavity in the defect metastrip: the hollow pillars to the right of the cavity are almost not vibrating. Reflection of incident Lamb waves occurs near the cavity, as illustrated by the inset of Fig. 4(c).

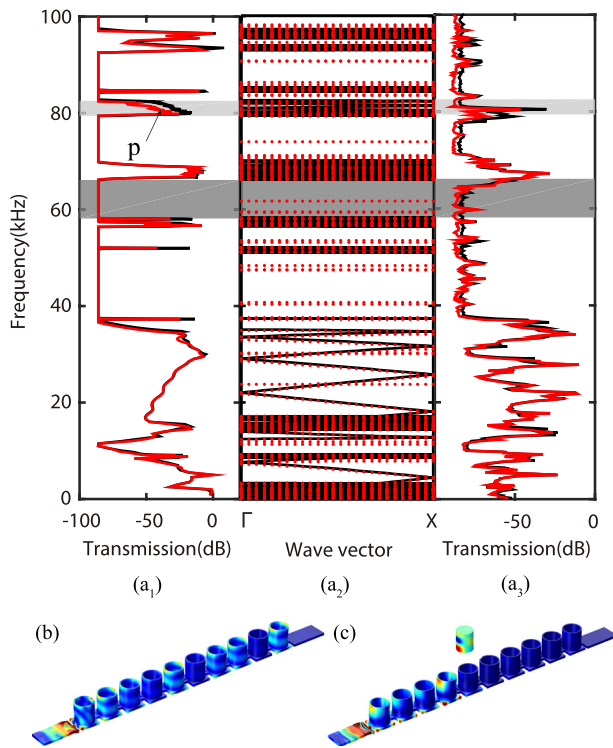


FIG. 4. Phononic band structure (a_2) and numerical (a_1) and experimental (a_3) transmission spectra for metastrips either without (black lines) or with the fifth pillar filled with water (red line and red dots). Band structures are obtained from a super-cell computation including 10 pillars. The distribution of total displacement at 81 kHz is shown in (b) without and (c) with the fifth pillar filled with water. The pressure distribution in water for the fifth pillar is presented as an inset in (c).

Finally, we increase the number of filled pillars in the metastrip and observe the changes in the spectral transmission. Figure 5 compares the numerical and experimental transmissions for 0, 3, 7, and 10 filled pillars. With the increase in the number of filled pillars, a transmission band gradually appears in the frequency range [58.5 kHz–66 kHz], from high

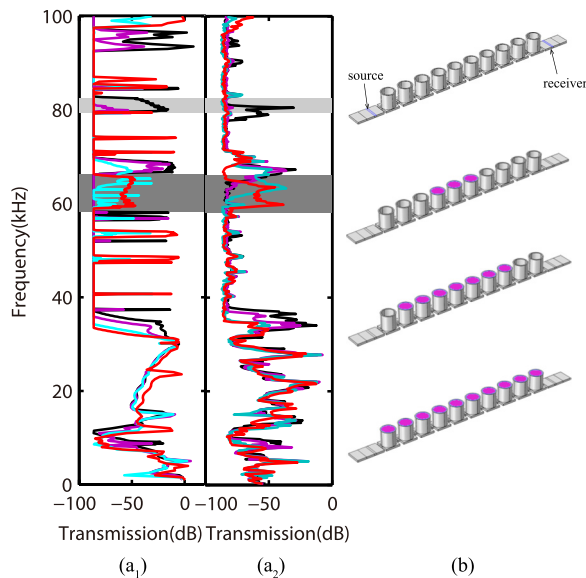


FIG. 5. Numerical (a_1) and experimental (a_2) transmission spectra for a finite metastrip with 0 (black line), 3 (purple line), 7 (blue line), and 10 (red line) pillars filled with water. The 4 configurations are depicted in panel (b). The pink and gray parts represent the water and aluminum, respectively.

to low frequencies. As a result, the bandgap switches to a passband gradually. Concurrently, transmission is gradually quenched in the frequency range [79.4 kHz–82.5 kHz] as more pillars are filled. This gives rise to a transition from a passband to a bandgap. Generally, tunability of the metastrip properties by filling water into the hollow aluminum pillars is observed to be a gradual process.

As a summary, we have demonstrated the tunability of a phononic metastrip whose hollow pillars can be filled with a fluid. Additional propagation modes are created owing to the fluid-solid interaction within the pillars. Transformation of a bandgap to a passband and the converse situation were both observed. Experimental results were found to agree satisfactorily with numerical results. The present work paves the way for the manipulation of Lamb waves.

The ideas in this letter can be directly extended to the 2D and 3D cases. Acoustic devices, such as coupled resonator acoustic waveguides^{27,30} or even more complicated circuits, can be designed. Assuming that the properties of fluids were tuned by external means,²⁷ tunable phononic circuits could be realized by filling the pillars with different fluids or different levels or gradient levels of the same fluid. Active or even smart manipulation of Lamb waves is thus expected.

Financial support by the National Natural Science Foundation of China (11642023 and 11532001) is gratefully acknowledged. The first two authors acknowledge the support from Fundamental Research Funds for the Central Universities (2016RC042 and 2017YJS149). V.L. acknowledges the financial support by Labex ACTION program (Contract No. ANR-11-LABX-0001-01).

¹M. S. Kushwaha, P. Halevi, L. Dobrzynski, and B. Djafari-Rouhani, *Phys. Rev. Lett.* **71**, 2022 (1993).

²Y. Tanaka and S.-I. Tamura, *Phys. Rev. B* **58**, 7958 (1998).

³Y. Pennec, B. Djafari-Rouhani, H. Larabi, J. Vasseur, and A.-C. Hladky-Hennion, *Phys. Status Solidi C* **6**, 2080 (2009).

⁴J.-H. Sun and T.-T. Wu, *Phys. Rev. B* **74**, 174305 (2006).

⁵Y. Pennec, B. Djafari-Rouhani, J. Vasseur, A. Khelif, and P. A. Deymier, *Phys. Rev. E* **69**, 046608 (2004).

⁶P. Alivisatos, *Nat. Biotechnol.* **22**, 47 (2004).

⁷R. Lucklum and J. Li, *Meas. Sci. Technol.* **20**, 124014 (2009).

⁸F.-L. Hsiao, A. Khelif, H. Moubchir, A. Choujaa, C.-C. Chen, and V. Laude, *Phys. Rev. E* **76**, 056601 (2007).

⁹T.-T. Wu, W.-S. Wang, J.-H. Sun, J.-C. Hsu, and Y.-Y. Chen, *Appl. Phys. Lett.* **94**, 101913 (2009).

¹⁰S. Mohammadi, A. A. Eftekhar, W. D. Hunt, and A. Adibi, *Appl. Phys. Lett.* **94**, 051906 (2009).

¹¹E. Coffy, T. Lavergne, M. Addouche, S. Euphrasie, P. Vairac, and A. Khelif, *J. Appl. Phys.* **118**, 214902 (2015).

¹²Y. Yao, F. Wu, X. Zhang, and Z. Hou, *Phys. Lett. A* **376**, 579 (2012).

¹³H. Khales, A. Hassen-Bey, and A. Khelif, *J. Vib. Acoust.* **135**, 041007 (2013).

¹⁴M. I. Hussein, G. M. Hulbert, and R. A. Scott, *J. Sound Vib.* **307**, 865 (2007).

¹⁵Y. Cheng, X. Liu, and D. Wu, *J. Acoust. Soc. Am.* **129**, 1157 (2011).

¹⁶F.-C. Hsu, C.-I. Lee, J.-C. Hsu, T.-C. Huang, C.-H. Wang, and P. Chang, *Appl. Phys. Lett.* **96**, 051902 (2010).

¹⁷Y. Pennec, B. D. Rouhani, C. Li, J. Escalante, A. Martínez, S. Benchabane, V. Laude, and N. Papanikolaou, *AIP Adv.* **1**, 041901 (2011).

¹⁸D. Hatanaka, I. Mahboob, K. Onomitsu, and H. Yamaguchi, *Nat. Nanotechnol.* **9**, 520 (2014).

¹⁹E. Coffy, S. Euphrasie, M. Addouche, P. Vairac, and A. Khelif, *Ultrasonics* **78**, 51 (2017).

²⁰Y. Pennec, B. D. Rouhani, H. Larabi, A. Akjouj, J. Gillet, J. Vasseur, and G. Thabet, *Phys. Rev. B* **80**, 144302 (2009).

²¹T.-C. Wu, T.-T. Wu, and J.-C. Hsu, *Phys. Rev. B* **79**, 104306 (2009).

- ²²C. Ma, J. Guo, and Y. Liu, *J. Phys. Chem. Solids* **87**, 95 (2015).
- ²³T. D. Ha and J. Bao, *AIP Adv.* **6**, 045211 (2016).
- ²⁴A. Khelif, A. Choujaa, S. Benchabane, B. Djafari-Rouhani, and V. Laude, *Appl. Phys. Lett.* **84**, 4400 (2004).
- ²⁵F. Casadei and K. Bertoldi, *J. Appl. Phys.* **115**, 034907 (2014).
- ²⁶Y. Jin, Y. Pennec, Y. Pan, and B. Djafari-Rouhani, *Crystals* **6**, 64 (2016).
- ²⁷Y.-F. Wang, T.-T. Wang, Y.-S. Wang, and V. Laude, *Phys. Rev. Appl.* **8**, 014006 (2017).
- ²⁸Y. Jin, N. Fernandez, Y. Pennec, B. Bonello, R. P. Moiseyenko, S. Hémon, Y. Pan, and B. Djafari-Rouhani, *Phys. Rev. B* **93**, 054109 (2016).
- ²⁹Y.-F. Wang, Y.-S. Wang, and V. Laude, *Phys. Rev. B* **92**, 104110 (2015).
- ³⁰J. M. Escalante, A. Martínez, and V. Laude, *J. Phys. D: Appl. Phys.* **46**, 475301 (2013).